Microwave-Assisted Synthesis and Magnetic Study of Nanosized Ni/NiO Materials

Carmen Parada and Emilio Morán*

Departamento de Química Inorgánica, Facultad de Ciencias Químicas, Universidad Complutense, 28040 Madrid, Spain

Received May 30, 2005. Revised Manuscript Received April 3, 2006

By using a domestic microwave furnace and depending on the nickel precursor used, either tetrahydrated nickel acetate or dihydrated nickel formate, different nanosized materials are obtained: Ni/NiO composites, Ni metal, or NiO. The acetate leads to core−shell composites: Ni on the outside and NiO on the inside, while the formate behaves oppositely, yielding the metal that is progressively oxidized in air, the shell being in this case NiO. All these materials show ferromagnetic behavior.

Introduction

Nanosized materials are known to exhibit profound changes in properties in comparison to those of bulk single crystals, microcrystalline powders, or thin films with the same chemical composition. Nowadays, there is an increasing interest in nanomaterials (nanoparticles, nanostructured matter, etc.) for fundamental scientific reasons and potential applications as well: catalysis, magnetic recording, etc. On these grounds, in the past few years, different methods for the preparation of nanoparticles, which can be classified as chemical, mechanochemical, and thermochemical, are being explored.[1−4]

Within the thermophysical methods, the use of microwave irradiation for the synthesis and processing of materials is an exciting new field with enormous potential. Because of the high penetration depth of microwaves, this way of heating is very fast and uniform, thermal gradients are minimized, the time for particle diffusion is reduced, and hence, the products can be obtained in a relatively short time; moreover, sintering of the particles is not favored, and therefore, small particles sizes can be achieved. Because of all these advantages, microwave synthesis is becoming quite common in the organic, biochemical, or pharmaceutical laboratories,[5−7] but its scope and use in inorganic solid-state synthesis is more restricted, probably because of the limited availability of adequate microwave susceptors. Nevertheless, the synthesis of some inorganic materials by using microwaves has been found to be advantageous in terms of energy saving, shorter processing times, uniformity of products, and reduction of particle size.[8−14]

One of the materials that undergoes dramatic property changes when the particle size is varied is NiO, especially its electrical and magnetic properties. Hence, stoichiometric NiO shows a very low electrical conductivity, less than 10^{-13} Ω^{-1} cm^{-1} at room temperature, and is classified as a Mott−Hubbard insulator,[15,16] but the conductivity increases 6−8 orders of magnitude in nanosized NiO as compared to that of single crystals, something that is attributed to the high density of defects induced by these means.[17,18] Concerning the magnetic properties, single crystals of NiO are antiferromagnetic (AF), the Néel temperature being 523 K, but when the crystallite sizes are of the order of a few nanometers, they become superparamagnetic (SPM) or superantiferromagnetic (SAFM).[19−25] Because of the interest in the application of nanosized metal oxides as anode materials for rechargeable batteries, ethanol fuel cells, and electrochemical capacitors, NiO is being intensively investigated, and it has been pointed out that electrodes composed of nanocrystalline NiO particles exhibit a higher capacity and better cyclability than the ordinary ceramic material.[26−29]

* Corresponding author. E-mail: emoran@quim.ucm.es.

(1) Rodríguez Paez, J. E.; Caballero, A. C.; Villegas, M.; Moure, C.; Durán, P.; Fernández, J. F. *J. Eur. Ceram. Soc.* **2002**, *21*, 925.
(2) Alymov, M. I.; Leontieva, O. N. *Nanostruct. Mater.* **1997**, *9*, 291.
(3) Porta, F.; Recchia, S.; Bianchi, C.; Confalorieri, F.; Scari, G. *Colloids Surf. Phys. Eng. Aspects* **1999**, *155*, 395.
(4) Livalyn, P. L.; Chevrot, V.; Ragail, J.; Cerlier, O.; Estienne, J.; Rouquerol, F. *Solid State Ionics* **1997**, *101−103*, 1293.
(5) Whitefield, P. S.; Davidson, J. J. *J. Electrochem. Soc.* **2000**, *147*, 4476.
(6) Swain, B. *Adv. Mater. Processes* **1986**, *134*, 76.
(7) Nüchter, M.; Ondruchka, B.; Bonrath, W.; Gumm, A. *Green Chem.* **2004**, *6*, *128*.
(8) Lewis, D.; Rayne, R. J.; Bender, D. A.; Kurihara, L. K.; Chow, G. M.; Fliffet, A.; Kincaid, A.; Bruce, R. *Nanostruct. Mater.* **1997**, *91*, 9.
(9) Wang, G.; Wittaker, G.; Harrisson, A.; Song; L. *Mater. Res. Bull.* **1998**, *33*, 1571.
(10) Caillot, T.; Aynes, D.; Stuerg, D.; Viart, N.; Perrouy, G. *J. Mater. Sci.* **2002**, *37*, 5153.
(11) Sankaranayanan, V. K.; Sreekmma, C. *Curr. Appl. Phys.* **2000**, *3*, 205.
(12) Xue-Hong, L.; Vian-You, C.; Shu, X.; Shui, B.; Jun-jie, Z. *J. Cryst. Growth* **2003**, *252*, 593.
(13) Harpeness, R.; Gedanke, A. *New J. Chem.* **2003**, *27*, 1191.
(14) Ying, J.; Wei-Wei, W.; Rui-Juan, Q.; Xian-Luo, H. *Angew. Chem., Int. Ed.* **2004**, *43*, 1410.
(15) Morin, F. G. *Phys. Rev. B* **1954**, *93* (6), 1199.
(16) Lukenheimer, P.; Wide, A.; Ottermann, C. R.; Bange, K. *Phys. Rev. B* **1991**, *44* (11), 5927.
(17) Biju, V.; Khadar, A. M. *J. Mater. Sci.* **2003**, *38*, 4005.
(18) Biju, V.; Khadar, A. M. *J. Mater. Sci.* **2001**, *36*, 5779.
(19) Makhlouf, S. A.; Parker, F. T.; Spada, F. E.; Berkovich, A. E. *J. Appl. Phys.* **1997**, *81*, 1997.
(20) Kilcoyne, S. H.; Cyminski, R. *J. Magn. Magn. Mater.* **1995**, *140−141*, 1446.
(21) Khadar, A. M.; Biju, V.; Ivanove, A. *Mater. Res. Bull.* **2003**, *38*, 1341.
(22) Pejova, B.; Kokareva, T.; Nadjoski, R.; Groddanov, I. *Appl Surf. Sci.* **2000**, *165*, 271.
(23) Biju, V.; Khadar, M. A. *Mater. Sci. Eng.* **2001**, *304−306*, 804.
(24) Kodama, R. H. *J. Magn. Magn. Mater.* **2000**, *221*, 32.
(25) Besenhard, J. O.; Yang, J.; Winter, M. *J. Power Sources* **1997**, *68*, 87.

10.1021/cm0511365 CCC: $33.50
Published on Web 05/05/2006

On the other hand, nanosized ferromagnetic (FM) metals (Fe, Co, and Ni) are also being widely studied as they present both an interest for fundamental physics[30−34] and an interest for applications such as magnetic storage, ferrofluids, medical diagnosis, multilayer capacitors, and catalysis.[35−44] Although a wide variety of techniques has been used to produce either nickel or nickel oxide nanoparticles (i.e., sonochemical),[45−46] sol−gel,[47−50] spray pyrolysis,[51,52] laser ablation,[53] thermal decomposition,[54−56] high energy ball milling,[57,58,59] and sputtering methods[60] the synthesis of these materials by using microwave irradiation is scarce.[61]

Taking all this into account, the aim of this work has been to produce nanosized particles of nickel oxide, nickel metal, or NiO/Ni composites by using microwave radiation and to study their magnetic behavior.

Experimental Procedures

The reagents used in this study were analytical grade purity: nickel acetate, $Ni(CH_3\text{-}COO)_2 \cdot 4H_2O$, or nickel formate, $Ni(COO)_2 \cdot 2H_2O$, and carbon black (added to enhance microwave absorption). Different weight percentages of carbon black were added to the respective nickel salts (5%C, 10%C, and 15%C) and then mechanically homogenized and compacted in pellets of a 12 mm diameter. The pellets were put in an alumina crucible and placed inside another larger one stuffed with mullite. The purpose of using mullite is to maintain the same position of the pellets in each experiment and to avoid the breaking or cracking of the glass turntable. The whole assembly was kept at the center of the turntable, and the microwave processing was carried out for periods of 5, 10, 15, and 30 min each. Worth noting: the microwave source is a domestic microwave oven, operating at a 2450 MHz frequency and 1000 W power. The choice of the nickel precursors was based on several requirements: (a) sufficiently high electrical permittivity, (b) noncentrosymmetrical structure, and (c) simple composition and availability.

Powder X-ray diffraction (XRD) was used to characterize the samples. Data were collected on a Phillips X-Pert X-ray diffractometer (Cu K_α radiation, $\lambda = 1.5418$ Å), filtered with nickel. Morphologies and sizes were observed by means of transmission electron microscopy (TEM) performed on a JEOL transmission electron microscope, using an accelerating voltage of 200 KV. The average size of the particles was also calculated from the full width at half-maximum (FWHM) of relevant peaks using the Scherrer equation,[62] which is given by $X_s = 0.9\lambda/\text{FWHM} \cos\theta$, where χ_s is the crystallite size, λ is the X-ray wavelength, and θ is the diffraction angle.

Magnetic measurements were performed on a SQUID magnetometer (Quantum Design). M/H measurements were made with applied fields up to 5 T, and in some cases, the complete hysteresis loops, characteristic of ferromagnetic behavior, were recorded. Zero-field-cooling (ZFC) and field-cooling (FC) experiments in an applied field of 1000 G were also performed to measure the temperature dependence of the magnetization between 5 and 300 K.

The values of the specific areas were measured by the BET method and calculated from the corresponding nitrogen adsorption isotherms at 77 K, using a Micrometrics ASAP 200 surface analyzer; a value of 0.164 nm^2 for the cross-section of the nitrogen molecule was used.

Results and Discussion

Nickel Acetate as Precursor. Two pathways were followed for the microwave irradiation: (a) keeping 15 min as a constant time and varying the amount of carbon (5−15%) and (b) fixing the amount of susceptor (10% weight of carbon) and varying the time of treatment from 5 to 60 min. In all the experiments carried out, the obtained products were nanosized nickel oxide/nickel metal composites in different ratios, depending on the amount of carbon black and the time of irradiation as illustrated by the XRD patterns of Figures 1 and 2.

If the amount of carbon black is 5%, the X-ray diffraction pattern (Figure 1, sample 1a) clearly shows the (111), (200), and (220) reflections of cubic NiO (JCPDS card no. 47-1049) as the main phase (aprox. 80%), besides the (111) and (200) peaks corresponding to fcc metallic nickel (JCPDS card no. 4-0850) as a second phase (∼ 20%). As the amount of carbon black increases (10% C), the ratio of intensities of the XRD

(26) Courney, L. A.; Dhan, J. R. *J. Electrochem. Soc.* **1997**, *1448*, 2943.
(27) Poizot, P.; Larnelle, S.; Grugeon, S.; Dupont, L.; Tarascon, J. M. *Nature* **2000**, *407*, 496.
(28) Cordente, N.; Touston, B.; Clollière, V.; Amiens, C.; Chaudret, B.; Verelest, M.; Respaud, M.; Broto, J. M. *C. R. Acad. Sci.* **2001**, *4*, 143.
(29) Fei-bao, Z.; Ying-ke, Z.; Hu-liu, L. *Mater. Chem. Phys.* **2004**, *83*, 60.
(30) Chen, J. P.; Sorensen, K. J.; Blabunde, J.; Hadpanayis, C. M. *Phys. Rev. B* **1995**, *51*, 11527.
(31) Gangopadnyay, S.; Hadjipanayis, C. M.; Sorensen, K. J.; Klabunde, J. *J. Appl. Phys.* **1993**, *73*, 6994.
(32) Chen, C.; Kitakania, O.; Shimada, Y. *J. Appl. Phys.* **1998**, *84*, 2134.
(33) Kodama, R. H. *J. Magn. Magn. Mater.* **1999**, *200*, 359.
(34) Aigh, T.; Meyer, P.; Lenerle, S. *Phys. Rev. Lett.* **1998**, *81*, 5656.
(35) Zhang, P.; Zuo, F.; Urban, F.; Khabai, A.; Griffiths, A.; Hosseini-Tehrani, J. *J. Magn. Magn. Mater.* **2002**, *225*, 371.
(36) Tseng, W.; Hsu, C.; Chi, C.; Teng, K. *Mater. Lett.* **2002**, *52*, 313.
(37) Schultz, L.; Schnike, K.; Wecker, J. *Appl. Phys. Lett.* **1990**, *56*, 868.
(38) Lu, L.; Sui, L.; Lu, K. *Science* **2000**, *287*, 463.
(39) Ozaki, M. *Mater. Res. Bull.* **1990**, *29*, 35
(40) Geiter, H. *Nanostruct. Mater.* **1992**, *1*, 1.
(41) Pontes, V. F.; Krishnan, K. M.; Aliviatos, A. P. *Science* **2001**, *291*, 2115.
(42) Sun, S.; Murray, C. B.; Weller, D.; Folks, L.; Moser, A. *Science* **2001**, *287*, 1989.
(43) Toneguzzo, P.; Vian, O.; Acher, F.; Fievet-Vincent, A.; Fievet, F. *Adv. Mater.* **1998**, *10*, 1032.
(44) Chen, W.; Li, L.; Qi, J.; Gui, J. *J. Am. Ceram. Soc.* **1998**, *81* (10), 2751.
(45) Ayyappan, S.; Gopalan, R. S.; Subbama, G. N.; Rao, C. N. *J. Mater. Res.* **1997**, *12*, B98.
(46) Jiangong, L.; Yong, Q.; Xiuli, K.; Juanjuan, H. *Nanotechnology* **2004**, *15*, 982.
(47) Cíntora-González, O.; Estournes, C.; Richard Pionet, M.; Guille, J. L. *Mater. Sci. Eng., C* **2001**, *15*, 179.
(48) Duan, Y.; Li, J. *Mater. Chem. Phys.* **2004**, *87*, 452.
(49) Tao, D.; Wei, F. *Mater. Lett.* **2004**, *58*, 3226.
(50) Fonseca, F. C.; Goya, G. F.; Jardim, R. F.; Macillo, R.; Carreño, V. L.; Longo, E.; Leite, E. R. *Phys. Rev. B* **2002**, *66*, 104406.
(51) Che, S.; Takada, K.; Mizutami, N. *J. Mater. Sci. Lett.* **1998**, *17*, 1227.
(52) Wang, W. N.; Yoshifimi, I.; Wuled-Lengorro, I.; Okuyama, K. *Mater. Sci. Eng., B* **2004**, *111*, 69.
(53) Seto, K.; Koga, K.; Akinaga, H.; Takana, F.; Sakiyama, K.; Hirasawa, M.; Orii, T. *Appl. Phys. A* **2004**, *79*, 1165.
(54) Jacha, N.; Chen, Y.; Peng, X. *Chem. Mater.* **2004**, *16*, 3931.
(55) Bi, L.; Li, S.; Zhang, Y.; Youvei, D. *J. Magn. Magn. Mater.* **2004**, *277*, 363.
(56) Khadar, M. A.; Biju, V.; Inone, A. *Mater. Res. Bull.* **2003**, *38*, 1341.
(57) González, E. M.; Montera, M. I.; Cebollada, F.; de Julián, C.; Vicent, J. L.; González, J. M. *Europhys. Lett.* **1998**, *42*, 91.
(58) Doppiu, S.; Langlais, V.; Sort, J.; Suriñach, S.; Baró, M. D.; Zhang, Y.; Hadjinapayis, G.; Nogués, J. *Chem. Mater.* **2004**, *16*, 5664.
(59) Sort, J.; Nogués, J.; Amils, X.; Suriñach, S.; Muñoz, J. S.; Baró, M. D. *Appl. Phys. Lett.* **1999**, *75*, 3177.
(60) Gavirin, A.; Chen, C. L. *J. Appl. Phys.* **1993**, *73*, 6949.
(61) Palckik, O.; Avivi, S.; Pinket, G.; Gedanken, A. *Nanostruct. Mater.* **1998**, *11* (3), 415.
(62) Cullity, B. D. *Elements of X-ray Diffraction*; Addison-Wesley: Reading, MA, 1978.

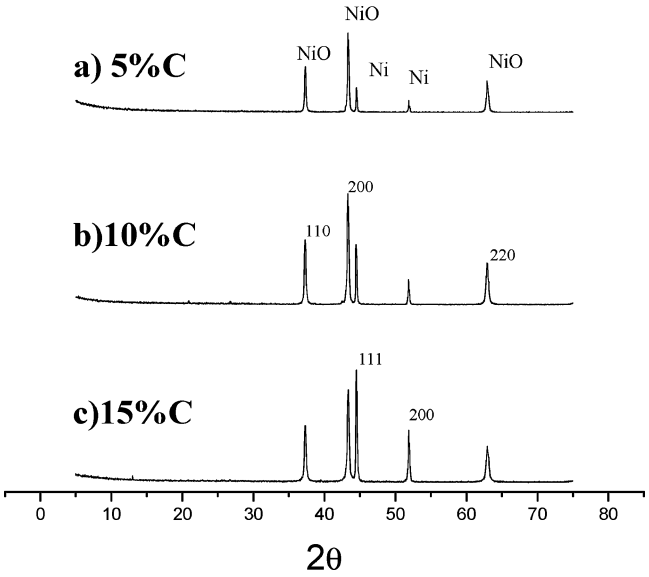

Figure 1. X-ray diffraction patterns of the materials obtained from nickel acetate mixed with different amounts of black carbon and irradiated for 15 min.

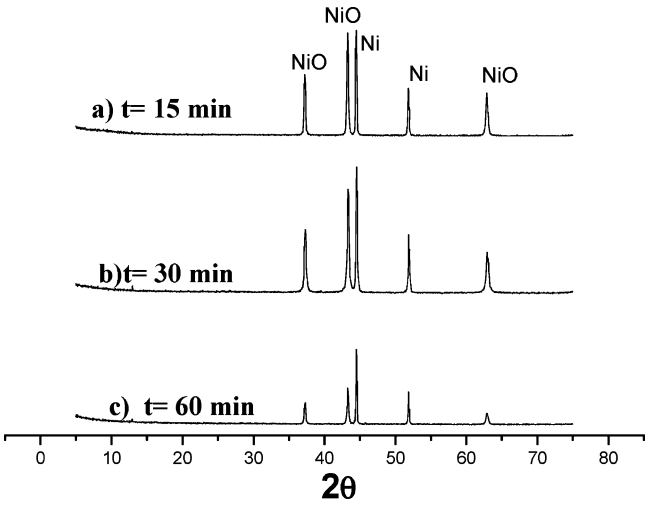

Figure 2. X-ray diffraction patterns of the materials obtained from nickel acetate mixed with 10% of black carbon and microwaved for different times.

peaks changes (Figure 1, sample 1b), and finally, for 15% black carbon added, the major phase (~60%) is metallic nickel (Figure 1, sample 1c). By using the Debye−Scherrer equation, the estimated average sizes of the particles range between 30 and 40 nm.

Figure 2 shows, through the corresponding XRD patterns, the influence of time (15, 30, and 60 min) for a fixed amount of carbon added (10%). It can be observed that the amount of metallic nickel produced also increases with time up to 1 h of treatment (sample 2c), for which metallic nickel is the major phase and the system does not evolve upon longer times of treatment. The relative visually estimated proportions of NiO/Ni are 50:50 (sample 2a); 60:40 (sample 2b); and 75:25 (sample 2c), and the average crystallite sizes are also between 30 and 40 nm.

On the other hand, Figure 3 shows a micrograph of a selected sample, 1b. Agglomerates of Ni/NiO are produced by the microwave-induced decomposition process, their grain size being nanometric. In the inset, the corresponding SAED

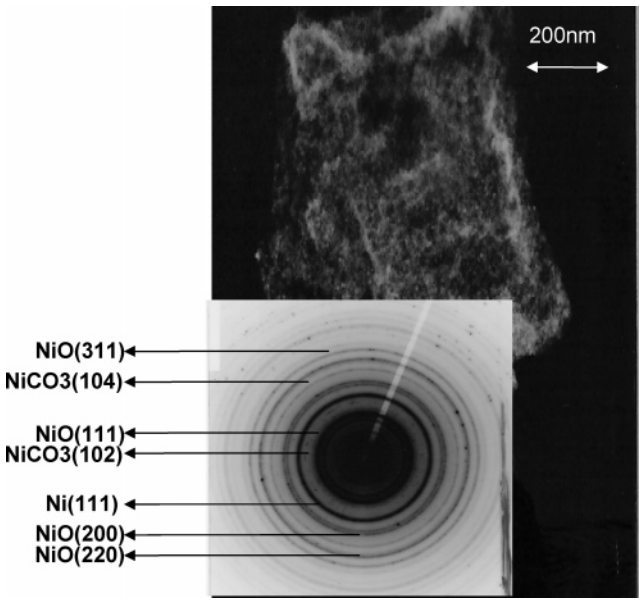

Figure 3. TEM, dark-field micrograph of sample 1b. The inset shows the corresponding SAED where different phases are identified.

pattern is depicted, showing the usual diffraction rings of a polycrystalline sample. This is in agreement with work reported by other authors on the thermal decomposition of nickel acetate, which always results in metallic nickel together with the expected nickel oxide although in different proportions depending on the atmosphere used.[63,64] This behavior is in contrast with the thermal decomposition of other nickel compounds (nitrate and hydroxide), which yields pure NiO. Interestingly enough, in this selected area of the sample, besides the characteristic peaks of NiO and Ni, we can also observe, as quite faint rings, the more intense diffraction peaks, (102) and (104) of $NiCO_3$, (JCPDS card no. 10-0272), formed as an intermediate product. The fact that the carbonate is not observed by means of XRD can be attributed to its concentration being below the detection limit. Nevertheless, it is worth showing, as it illuminates the decomposition mechanism.

Worth noting, the tetrahydrated nickel acetate is a molecular solid in which structure Ni is octahedrally coordinated, fully surrounded by oxygen, four of them belonging to the water and the other two to the acetates, which are monodentate ligands. Thus, the compound is better described as tetra-aqua-bis (acetato-oxygen)-nickel (II),[65] and although the thermal decomposition is quite complicated,[66] it is not surprising to find nickel oxide as the major product of the decomposition. Thus, the chemical decomposition processes induced in our case by the microwave irradiation are not very different from those produced by the conventional thermal heating, but times of treatment are much smaller, and the nanometric particle size is due to the lack of sintering; agglomerates are formed due to magnetic interaction between particles.

(63) Gadalla, A. H.; Yu, H.-F. *Thermochim. Acta* **1990**, *164*, 21.
(64) Estellé, J.; Salagre, P.; Cesteros, Y.; Serra, M.; Medina, F.; Sueiras, J. E. *Solid State Ionics* **2003**, *156*, 233.
(65) Cramer, R. E.; van Doome, W.; Dubois, R. *Inorg. Chem.* **1975**, *14*, 2462.
(66) Cerc Korosêc, R.; Bukovec, P. *Thermochim. Acta* **2004**, *410*, 65.

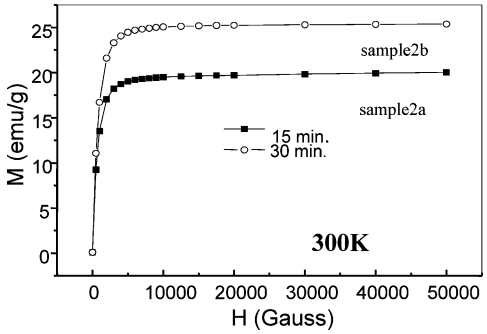

Figure 4. Magnetization vs applied field, measured at room temperature, corresponding to samples 2a and 2b. An increasing Ni/NiO ratio produces bigger magnetization.

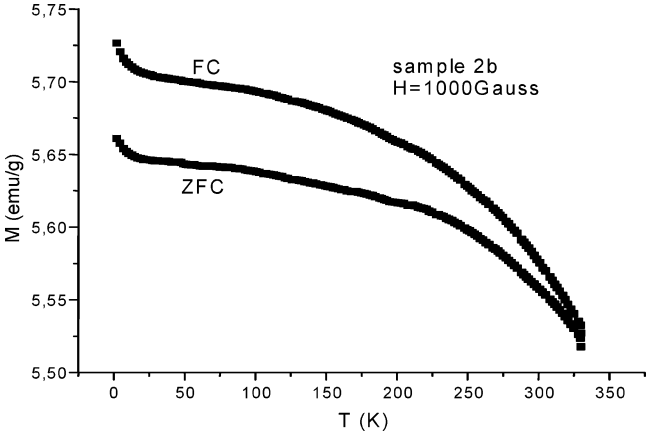

Figure 5. Field-cooled and zero-field-cooled magnetization vs temperature of sample 2b measured at 1000 G.

As regarding the magnetic properties, Figure 4 shows the magnetization versus applied field measured at room temperature of two composites (samples 2a and 2b) obtained with different times of microwave irradiation: $t = 15$ and $t = 30$ min, respectively. It can be seen that both samples saturate with M_s values of 20 and 25 emu/g, respectively. Assuming a ferromagnetic behavior close to that of the bulk metal for which a M_s value of 55 emu/g has been proposed,[67] we can estimate the amount of nickel in each sample, approximately 37 and 46%, respectively, in fairly good agreement with the proportions estimated from the intensities of the respective peaks in their XRD patterns (see Figure 2). To asses the possible superparamagnetism of these NiO/Ni composites that would appear as a result of the nanometric size of the particles,[28,47,50,56,67] we have performed measurements of the magnetization versus temperature of a representative material (sample 2b: 10% C, 30 min of treatment), cooling it within an applied magnetic field of 1000 G (FC measurements) and without it (ZFC measurements), as shown in Figure 5. In this plot, there is not a cusp in the ZFC plot, which discards superparamagnetic behavior.

Instead, we can observe that both curves (FC and ZFC) have the same shape and do not coincide, something characteristic of ferromagnetic materials. Moreover, some complete hysteresis loops (M vs H) have been obtained for the same sample at different temperatures (2, 75, and 200 K), which are shown in Figure 6; we can observe that the

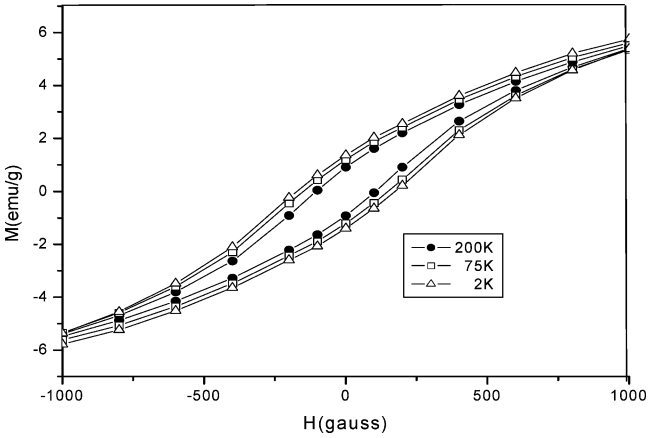

Figure 6. Hysteresis M/H loops at different temperatures corresponding to sample 2b.

values obtained at different temperatures are quite similar and that the shapes of the respective loops are quite symmetrical, something that can, indeed, be attributed to ferromagnetism. Thus, it can be concluded that, despite the nanometric size of our particles, no superparamagnetism is observed and that the ferromagnetic behavior of metallic nickel is the predominant feature.

Nickel Formate as Precursor. If the precursor employed is $Ni(CHO)_2 \cdot 2H_2O$ and following the same methodology previously described for nickel acetate (different amounts of carbon black or different times of irradiation), the microwave treatment only produces amorphization, independently either of the amount of carbon black added or the time of exposure. These amorphous phases are easily transformed to Ni → Ni/NiO → NiO nanosized phases at a moderate temperature and short heating times when treated in a conventional oven.

Thus, when the amorphous product is treated at 300 °C for 15 min, pure nickel is obtained; for longer treatments, 1−4 h, the obtained products are nanosized nickel/nickel oxide composites in different ratios. Finally, for longer heating times (i.e., 6 h), the product is nanosized NiO. Figure 7 shows the XRD patterns corresponding to four different samples heated for 15 min (Figure 7a), 1 h (Figure 7b), 3 h (Figure 7c), and 6 h (Figure 7d), where the more intense diffraction peaks corresponding to fcc cubic metallic nickel and nickel oxide can be observed with different relative intensities corresponding to the different phase proportions. In Table 1, the compositions and average size, determined using the full width at half-maximum (FWHM) of more intense peaks for samples 7a, 7c, and 7d, are listed. A remarkable feature regarding the particle size is the fact that the materials obtained upon oxidation are of smaller size than that of the precursor metallic nickel, meaning that the external shell is progressively being peeled off.

According to these results, it is possible to infer that the chemical process that takes place when using nickel formate occurs through an inverse path as compared to the nickel acetate case. The process can be described in three steps: (1) microwave heating: $Ni(HCO_2)_2 \cdot 2H_2O$ → amorphous phase; (2) short thermal treatment (air, 300 °C): amorphous phase → Ni (crystalline nanosized); and (3) long thermal

(67) Xia, B.; Lenggoro, I. W.; Okuyama, K. *J. Am. Ceram. Soc.* **2001**, *84* (7), 1425.

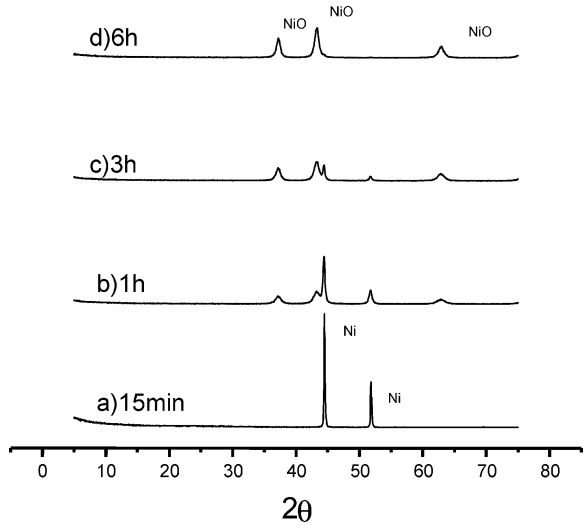

Figure 7. X-ray diffraction patterns of materials obtained from nickel formate after microwave irradiation and thereafter heated in air at 300 °C for 15 min (7a), 1 h (7b), 3 h (7c), and 6 h (7d).

Table 1. Summary of Microstructural Parameters of Phases Obtained from Nickel Formate as Precursor

sample	7a	7c	7d
Composition	Ni	Ni (40%) + NiO (60%)	NiO
Ø (nm) from XRD	37	19, 16	11
S_{BET} (m^2/g)	144	73	77

treatments (air, 300 °C): $Ni + 1/2O_2^- \rightarrow$ Ni O (crystalline nanosized).

The different response toward microwave irradiation of the formate and acetate precursors can be attributed to their different structure and bonding: the acetate is a molecular solid, as previously described, while in the formate structure, chains are formed because of the bridging character of the formate ligand, so that this salt should be named as catena tetra-aqua-tetrakis (μ_2 formate O,O′) dinickel (2).[68] The scheme presented is consistent with data reported by other authors,[69,70] which have prepared nickel powders by spray pyrolysis of nickel formate at 350 °C or nickel−nickel oxide nanoparticles by the same procedure from nickel nitrate and cosolvents such as formic acid; the thermal decomposition of the nickel formate proceeds in three steps: dehydratation, decomposition, and oxidation. It is worth recalling that in the past few years several attempts to produce nickel and nickel oxide nanoparticles in strong reducing conditions, such as working with hydrazine solutions, have been employed.[71−73] In our case, the formation of metallic nickel seems to be due to the reducing gases (H_2, CO) that the formates produce upon decomposition, and the nickel metal nanoparticles formed are highly reactive, and upon treatment in air, they are progressively oxidized to NiO, thus giving intermediate Ni/NiO nanosized composites when heating times are increased. Finally, after a long enough thermal treatment in air (6 h), they become monophasic NiO nanoparticles.

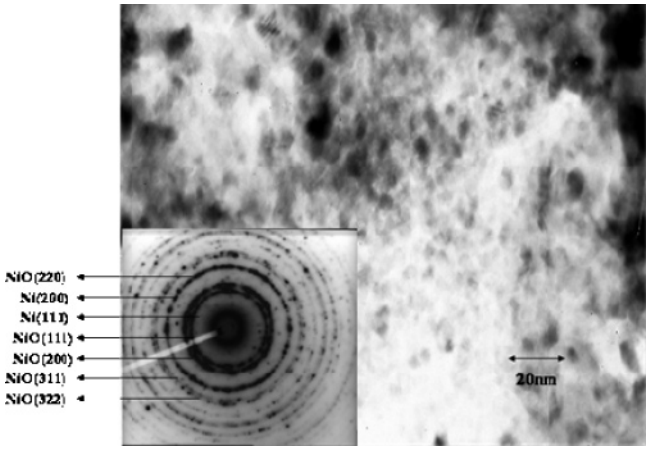

Figure 8. TEM bright-field and SAED pattern micrographs corresponding to sample 7c, a NiO/Ni composite.

In Table 1, the values of specific surface areas of some of the materials are also listed. It is worth noting that nickel obtained by this procedure (sample 7a) possesses a BET surface area of ≈144 m^2/g, higher than those reported for nickel Raney,[74] and thereafter, the oxidation of nickel gives nanosized nickel oxide (sample 7d) with a surface area approximately half of that of the parent nickel, but still quite high. Therefore, the use of these materials as catalysts in different processes should be explored.

Figure 8 shows a micrograph corresponding to a 3 h treated sample. It can be seen that the sizes of the particles are not homogeneous; ranging from ∼5 to ∼25 nm, the average size is of the order of 17 nm. The inset corresponds to the SAED pattern, where the typical rings of a polycrystalline sample are evident and have been indexed as (111) and (200) of fcc metallic nickel and (111), (200), and (220) of cubic NiO, although the intensities of rings are much weaker for the metal. As previously mentioned, longer treatments yield monophasic nanosized cubic NiO, and Figure 9 shows a micrograph corresponding to a 6 h treated sample. Interestingly, the size of these particles is smaller (≈10 nm), and the diffraction rings depicted in the inset correspond to polycrystalline cubic NiO.

Regarding the magnetic properties, bulk NiO is known to be an antiferromagnet with $T_N = 533$ K. However, when the particle size is only a few nanometers, the uncompensated magnetic spins associated with the surface atoms are not negligible and give rise to a net magnetization. In this connection, Figure 10 shows the magnetization versus applied field recorded at 2 K corresponding to a sample heated during 6 h at 300 °C in air that is quite pure NiO. A hysteresis loop is evident, consistent with ferromagnetic behavior (FM), in agreement with previous observations.[19,75,76] An extrapolated value at zero-field of 0.008 μ_B per Ni atom, equivalent to 0.60 emu/g, is reached at 2 K. Nevertheless, the magnetization does not saturate, even for

(68) Krogmann, K.; Mattes, R. *Z. Kristallogr.* **1963**, *118*, 291.
(69) Kang, D. J.; Kim, S. G.; Kim, H. S. *J. Mater. Sci.* **2004**, *39* (18), 5719.
(70) Wang, W. N.; Itoh, Y.; Lenggoro, I. V. *Mater. Sci. Eng., B* **2004**, *111* (1), 69.
(71) Boudjahem, A. G.; Monteverdi, S.; Mercy, M. *Langmuir* **2004**, *20* (1), 208.
(72) Wu, S. H.; Chen, D. H. *J. Colloid Interface Sci.* **2003**, *259* (2), 282.
(73) Mi, Y. Z.; Yuan, D. S.; Li, Y. L. *Mater. Chem. Phys.* **2005**, *89* (2−3), 359.
(74) Al-Saleh, M. A.; Sleem-Ur-Rahman, J. *Power Sources* **1998**, *72* (2), 159.
(75) Shuele, W. J.; Deetscreek, U. D. *J. Appl. Phys.* **1962**, *33*, 1136.
(76) Singer, J. R. *Phys. Rev.* **1956**, *104*, 929.

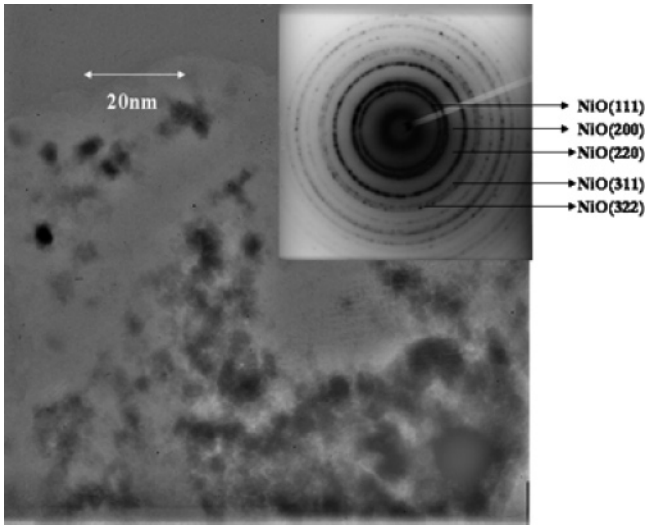

Figure 9. TEM bright-field and SAED pattern micrographs corresponding to sample 7d, pure NiO.

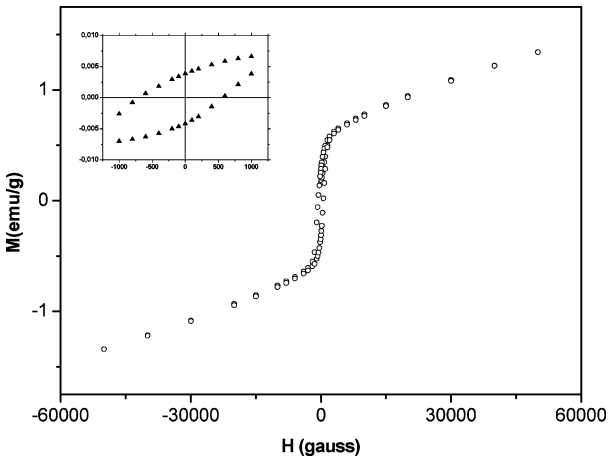

Figure 10. M/H meausurements at 2 K corresponding to sample 7d (NiO). The amplified hysteresis loop is shown in the inset.

an applied field of 5 T, and a coercitive field of ∼700 Oe can be measured at 2 K (see the inset). Interestingly enough, other authors have reported similar magnetization values for nanosized nickel oxide: ∼2.5 emu/g for particles of sizes about 2−3 nm and ∼0.3 emu/g for particles ranging between 13 and 18 nm;[21] the particle size being in our case about 10 nm.

On the other hand, for a sample that is pure metallic nickel (sample 7a), obtained by heating the amorphous phase at 300 °C for 15 min, FM behavior, as expected, has been found; see Figure 11.

In this case, a saturation magnetization value of 36 emu/g is reached at 6 T, smaller than that expected for ordinary, ferromagnetic nickel (55 emu/g), which can be related to the small size of the obtained nickel particles. Worth noting, these particles remain unaltered in room conditions at least for 3 months, which indicates that some passivation takes place.

In Ni/NiO composites such as sample 7b, obtained by heating the microwaved product for 1 h at 300 °C in air, and probably with a core−shell configuration, ferromagnetism is also observed, and moreover, a very interesting new phenomenon, referred to in the literature as an exchange

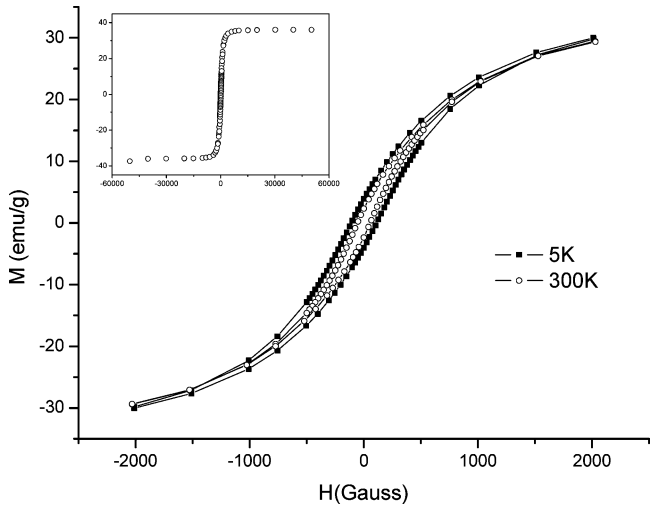

Figure 11. Magnetization hysteresis loops observed at 5 and 300 K for sample 7a (pure Ni). The inset shows the M/H measurements up to 6 T at 300 K.

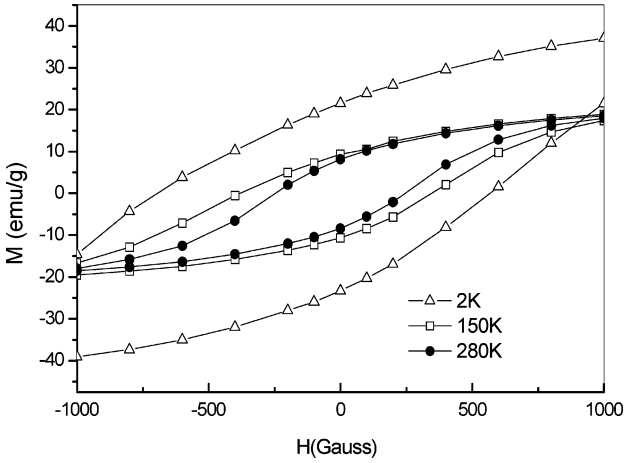

Figure 12. Asymmetrical hysteresis loops observed in M vs H measurements for sample 7b (Ni/NiO composite) at different temperatures: 2, 150, and 280 K.

bias, can be detected. This phenomenon, typical of the interaction between ferromagnetic−antiferromagnetic materials, has been extensively studied in nanostructures by Nogués et al.[78] and consists of a displacement along the magnetic field axis of the hysteresis loops, which become asymmetric. In this connection, we have measured different hysteresis loops on the magnetization curves at $T = 2$, 150, and 280 K, which are shown in Figure 12. It can be observed that the coercivity H_C reduces with temperature (∼650, ∼450, and ∼250 Oe at 2, 150, and 280 K, respectively), a feature that can be attributed to the role of thermal activation as it occurs in ferromagnetic materials when approaching the Curie temperature. It can be seen that the hysteresis loops presented are somehow asymmetric and shifted along the field axis, and therefore, an exchange bias is apparent in this material; it can be estimated as 50 G, and most likely, the FM material would be the nickel in the core of the particles while the AFM material would be the nickel oxide shell.[77]

(77) Seto, T.; Akinaga, H.; Takano, F.; Koga, K.; Orii, T.; Hirasava, M. J. *Phys. Chem. B* **2005**, *109* (28), 13403.
(78) Nogués, J.; Sort, J.; Langlais, V.; Skumryev, V.; Suriñach, S.; Muñoz, J. S.; Baró, M. D. *Phys. Rep.* **2005**, *422*, 65.

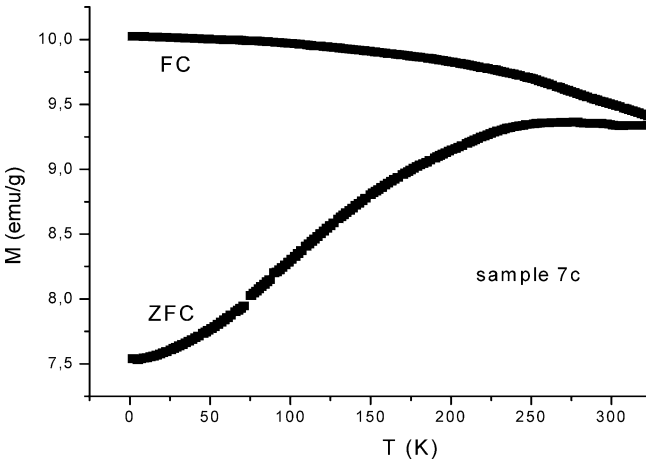

Figure 13. Zero-field-cooled and field-cooled measurements of the magnetization vs temperature in an applied field of 1000 G corresponding to a Ni/NiO composite (sample 7c). A cusp near 250 K in the ZFC plot is evident.

Actually, other authors have also found exchange bias effects in mixtures of Co (FM) and NiO (AFM) nanometric powders that, although prepared by a different method (high energy ball milling), show a quite similar microstructure.[59]

Finally, and to continue in the magnetic study of these materials and to compare them with those obtained in the decomposition of the acetate precursor, we have also performed magnetization versus temperature measurements in zero-field-cooled and field-cooled conditions: the results are shown in Figure 13, where a strong deviation between both curves is evident, and as an important feature to note, the M_{ZFC} curve exhibits a cusp at 250−300 K that defines the blocking temperature (T_B),[79] above which superparamagnetic (SPM) behavior is normally accepted. Again, this seems to be due to the small size of the particles (∼19 nm) when produced from the formate, very different from the acetate. More work at higher temperatures is in progress to ascertain this particular point.

Conclusion

As a summary, we can conclude that the microwave irradiation of two different nickel organic salts (acetate and formate) produces Ni/NiO nanoparticles but quite differently. The acetate directly produces particles (∼25 nm) of the antiferromagnetic oxide that are progressively reduced to ferromagnetic nickel. In the formate case, two consecutive treatments are required: microwave irradiation and then conventional thermal treatment in air, and this results in smaller nanoparticles (∼10 nm) where ferromagnetism is always observed: for pure NiO (normally antiferromagnetic), pure Ni, and Ni/NiO composites as well, which would present a core−shell morphology (nickel in the core and an oxide shell).

Acknowledgment. The authors express their gratitude to MCYT for financial support (Project MAT2004-03070-CO-05). Thanks are due to Dr. J. Velázquez (UCM Center for XRD), Dr. J. Romero (Magnetism), A. Gómez (UCM Microscopy Center), and Prof. M. J. Torralvo and Dr. M. C. Carbajo (Department of Inorganic Chemistry, S_{BET}) for performing different measurements. We are indebted to Profs. M. A. Alario-Franco and R. Sáez-Puche for helpful discussions.

CM0511365

(79) Stephen Blundell. *Magnetism in Condensed Matter*; Oxford University Press: New York, 2001.